Pro-cathepsin D interacts with the extracellular domain of the β chain of LRP1 and promotes LRP1-dependent fibroblast outgrowth

Mélanie Beaujouin[1–4], Christine Prébois[1–4], Danielle Derocq[1–4], Valérie Laurent-Matha[1–4], Olivier Masson[1–4], Sophie Pattingre[1–4], Peter Coopman[5], Nadir Bettache[5], Jami Grossfield[6], Robert E. Hollingsworth[6], Hongyu Zhang[7], Zemin Yao[7], Bradley T. Hyman[8], Peter van der Geer[9], Gary K. Smith[10] and Emmanuelle Liaudet-Coopman[1–4,*]

[1]IRCM, Institut de Recherche en Cancérologie de Montpellier, [2]INSERM, U896, [3]Université Montpellier 1, and [4]CRLC Val d'Aurelle Paul Lamarque, Montpellier, F-34298, France
[5]Centre de Recherche de Biochimie Macromoléculaire, CNRS UMR 5237, Université Montpellier 2, 34293 Montpellier Cedex 5, France
[6]Genetics Research, GlaxoSmithKline, Five Moore Drive, Research Triangle Park, NC 27709, USA
[7]Department of Biochemistry, Microbiology and Immunology, University of Ottawa, Ottawa K1Y4W7, Canada
[8]Alzheimer Disease Research Laboratory, Massachusetts General Hospital, Harvard Medical School, Charlestown, MA 02129, USA
[9]Department of Chemistry and Biochemistry, San Diego State University, 5500 Campanile Drive, MC 1030, San Diego, CA 92182-1030, USA
[10]Screening and Compound Profiling, GlaxoSmithKline, Five Moore Drive, Research Triangle Park, NC 27709, USA
*Author for correspondence (emmanuelle.liaudet-coopman@inserm.fr)

Accepted 24 May 2010
Journal of Cell Science 123, 3336-3346

doi:10.1242/jcs.070938

Summary

Interactions between cancer cells and fibroblasts are crucial in cancer progression. We have previously shown that the aspartic protease cathepsin D (cath-D), a marker of poor prognosis in breast cancer that is overexpressed and highly secreted by breast cancer cells, triggers mouse embryonic fibroblast outgrowth via a paracrine loop. Here, we show the requirement of secreted cath-D for human mammary fibroblast outgrowth using a three-dimensional co-culture assay with breast cancer cells that do or do not secrete pro-cath-D. Interestingly, proteolytically-inactive pro-cath-D remains mitogenic, indicating a mechanism involving protein-protein interaction. We identify the low-density lipoprotein (LDL) receptor-related protein-1, LRP1, as a novel binding partner for pro-cath-D in fibroblasts. Pro-cath-D binds to residues 349–394 of the β chain of LRP1, and is the first ligand of the extracellular domain of LRP1β to be identified. We show that pro-cath-D interacts with LRP1β in cellulo. Interaction occurs at the cell surface, and overexpressed LRP1β directs pro-cath-D to the lipid rafts. Our results reveal that the ability of secreted pro-cath-D to promote human mammary fibroblast outgrowth depends on LRP1 expression, suggesting that pro-cath-D–LRP1β interaction plays a functional role in the outgrowth of fibroblasts. Overall, our findings strongly suggest that pro-cath-D secreted by epithelial cancer cells promotes fibroblast outgrowth in a paracrine LRP1-dependent manner in the breast tumor microenvironment.

Key words: Cathepsin D, LRP1, Tumor microenvironment, Cancer, Fibroblast outgrowth

Introduction

Tumor progression has been recognized as the product of evolving crosstalk between tumor cells and the surrounding supportive tissue, known as the tumor stroma (Mueller and Fusenig, 2004). Cancer cells interact dynamically with several normal cell types within the extracellular matrix, such as fibroblasts, infiltrating immune cells, endothelial cells and adipocytes (Mueller and Fusenig, 2004). Stromal and tumor cells exchange enzymes, growth factors and cytokines that modify the local extracellular matrix, stimulate migration and invasion, and promote the proliferation and survival of stromal and tumor cells (Liotta and Kohn, 2001; Masson et al., 1998).

The aspartic protease cathepsin D (cath-D) is overexpressed and highly secreted by human epithelial breast cancer cells (Capony et al., 1989; Liaudet-Coopman et al., 2006; Rochefort and Liaudet-Coopman, 1999; Vignon et al., 1986). Its overexpression in breast cancer is correlated with poor prognosis (Ferrandina et al., 1997; Foekens et al., 1999; Rodriguez et al., 2005). Human cath-D is synthesized as a 52-kDa precursor that is rapidly converted in the endosomes to form an active, 48-kDa, single-chain intermediate, and then in the lysosomes into the fully active mature protease, composed of a 34-kDa heavy chain and a 14-kDa light chain. The human cath-D catalytic site includes two crucial aspartic residues (amino acids 33 and 231) located on the 14-kDa and 34-kDa chains, respectively (Metcalf and Fusek, 1993). The overexpression of cath-D in breast cancer cells leads to the hypersecretion of the 52-kDa pro-cath-D into the extracellular environment (Heylen et al., 2002; Laurent-Matha et al., 1998; Vignon et al., 1986). Secreted pro-cath-D can be endocytosed by both cancer cells and fibroblasts (Heylen et al., 2002; Laurent-Matha et al., 1998; Vignon et al., 1986), mainly via the mannose-6-phosphate receptors (M6PR) or by alternative cath-D receptors (Capony et al., 1994; Laurent-Matha et al., 2005; Rijnboutt et al., 1991). Cath-D affects both cancer cells and stromal cells in the tumor microenvironment by increasing cancer cell proliferation (Vignon et al., 1986; Glondu et al., 2001; Glondu et al., 2002; Berchem et al., 2002), metastasis (Glondu et al., 2002) and angiogenesis (Berchem et al., 2002; Hu et al., 2008); it was also found that cath-D increases the three-dimensional (3D) growth (outgrowth) of fibroblasts embedded in a Matrigel matrix (Laurent-Matha et al., 2005). We had previously

observed that a mutated catalytically inactive version of cath-D (D231N) remains mitogenic for tumor cells and mouse embryonic fibroblasts (Berchem et al., 2002; Glondu et al., 2001; Laurent-Matha et al., 2005), suggesting that cath-D acts as an extracellular messenger that interacts either directly or indirectly with an as-yet-unidentified cell surface receptor.

In the present study, we show that pro-cath-D hypersecreted by cancer cells stimulates the outgrowth of human mammary fibroblasts (HMFs) embedded in a Matrigel matrix, thus indicating for the first time the relevance of the paracrine role of secreted cath-D in a pathological context. We also identify the low-density lipoprotein (LDL) receptor-related protein-1 (LRP1) as a novel binding partner for cath-D in fibroblasts, and present data in support of a functional role for this interaction in the outgrowth of fibroblasts that is induced by epithelial cancer cells. LRP1 is composed of a 515-kDa extracellular α chain, and an 85-kDa β chain (Lillis et al., 2005; Strickland and Ranganathan, 2003). The extracellular α chain contains binding sites for many structurally unrelated ligands, including lipoprotein particles, proteases and protease–inhibitor complexes. The β chain contains an extracellular domain, a transmembrane region and a cytoplasmic tail. At present, the ligands of the extracellular domain of the LRP1β chain are still unknown. In this study, we report for the first time the interaction between pro-cath-D and the extracellular domain of the β chain of LRP1.

Results

Pro-cath-D secreted by cancer cells stimulates 3D outgrowth of HMFs

The communication between epithelial cancer cells and fibroblasts plays a crucial role in cancer progression. We had previously developed a 3D co-culture system showing that human breast cancer MCF-7 cells induce outgrowth of mouse embryonic, human skin, and breast fibroblasts, indicating that these epithelial cancer cells secrete paracrine factors capable of promoting fibroblast outgrowth in 3D matrices (Laurent-Matha et al., 2005). These factors included cath-D, and we demonstrated that secreted cath-D was involved in the outgrowth of mouse embryonic cath-D-deficient fibroblasts independently of its catalytic activity (Laurent-Matha et al., 2005).

In order to study the relevance of the paracrine role of secreted pro-cath-D in the context of human breast cancer, we have now performed our 3D co-culture system using HMFs (Fig. 1Aa). To find out whether secreted pro-cath-D might be one of the crucial paracrine factors affecting HMF outgrowth, 3D co-culture assays were carried out using MCF-7 cells (Fig. 1Ac) in which endogenous pro-cath-D secretion was reduced by 75% by small-RNA-mediated gene silencing (*cath-D* siRNA) for 2 days before the co-culture assay (Fig. 1Ad). MCF-7 cells transfected with *cath-D* siRNA (Fig. 1Ab, middle) were less effective in triggering HMF outgrowth than MCF-7 cells transfected with control luciferase siRNA (*luc* siRNA) (Fig. 1Ab, left). A 75% inhibition of pro-cath-D secretion by cells transfected with *cath-D* siRNA still occurred during our co-culture assay, even after 3 days of co-culture (Fig. 1Ad). By

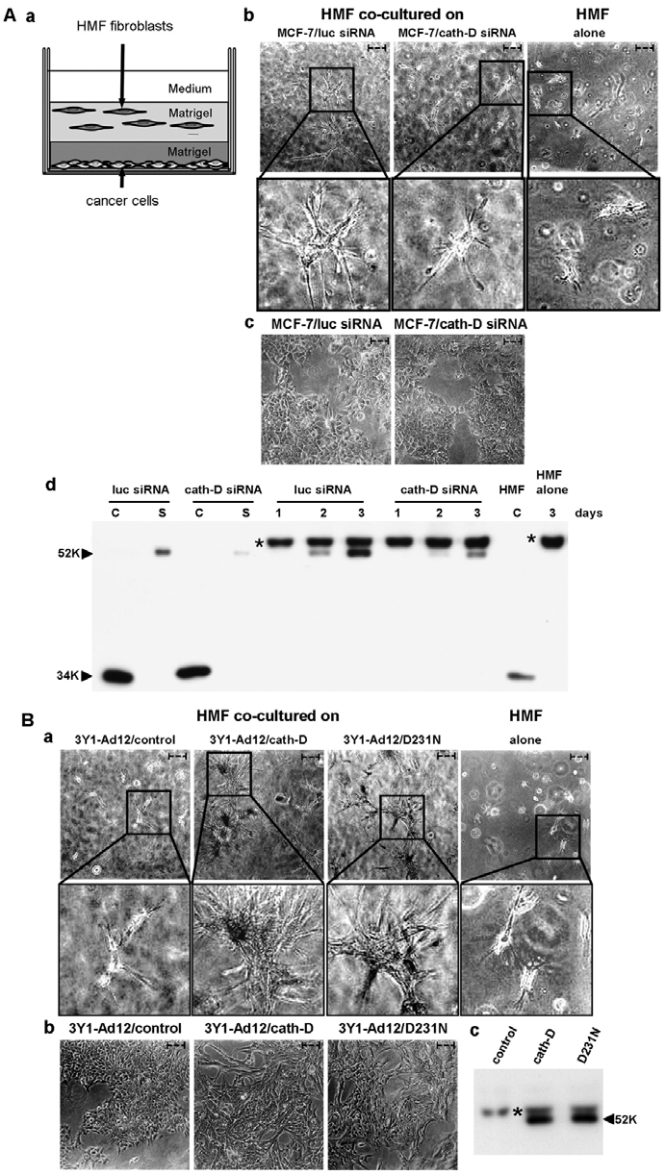

Fig. 1. Pro-cath-D secreted by cancer cells stimulates the 3D outgrowth of HMFs independently of its catalytic function. (**A**) Outgrowth of HMFs co-cultured with MCF-7 breast cancer cells in which pro-cath-D secretion was inhibited by siRNA silencing. HMFs were embedded in Matrigel with or without a bottom layer of MCF-7 cancer cells (panel a). Phase-contrast optical photomicrographs of HMFs embedded alone (panel b, right) or in the presence of a bottom layer of MCF-7 cells (panel b, left and middle) after 3 days of co-culture are shown. High magnifications of the boxed regions are displayed below. Phase-contrast optical photomicrographs of MCF-7 cells transfected with *cath-D* or *luc* siRNAs after 3 days of co-culture are presented (panel c). (Panel d) Expression and secretion of pro-cath-D were monitored in MCF-7 cell lysates (C) and media (S) before the beginning of the co-culture, and then in the media at day 1-3 of co-culture by western blot. Secretion of pro-cath-D was also monitored in media of HMF cells embedded alone at day 3 of co-culture (panel d). Expression of cath-D in a HMF lysate (C) is shown. (**B**) Outgrowth of HMFs co-cultured with 3Y1Ad12 cancer cells secreting no pro-cath-D, pro-cath-D or ^{D231N}pro-cath-D. HMFs were embedded with or without a bottom layer of 3Y1Ad12 cancer cell lines secreting no pro-cath-D (control), human wild-type (pro-cath-D) or D231N pro-cath-D (D231N) as described in A (panel a). Phase-contrast optical photomicrographs of HMFs after 3 days of co-culture are shown (panel a). High magnifications of the boxed regions are displayed below. Phase-contrast optical photomicrographs of 3Y1-Ad12 cancer cell lines after 3 days of co-culture are presented (panel b). Pro-cath-D secretion was analyzed after 3 days of co-culture by western blot (panel c). *Non-specific contaminant protein. K, molecular mass in kilodaltons. Scale bars: 50 μm.

contrast, in HMFs embedded alone (Fig. 1Ab, right), pro-cath-D secretion was not detected after 3 days of co-culture (Fig. 1Ad). We conclude that the inhibition of pro-cath-D secretion in breast cancer cells rapidly reduces HMF outgrowth.

To analyze the role of the catalytic activity of secreted pro-cath-D, we then carried out 3D co-culture assays with *cath-D*-transfected rat 3Y1-Ad12 cancer cell lines secreting either no human cath-D (control), or hypersecreting either human wild-type cath-D (cath-D) or D231N mutated cath-D devoid of proteolytic activity (D231N) (Fig. 1Bb). Only the 3Y1-Ad12 cancer cells secreting wild-type or D231N pro-cath-D (Fig. 1Bc) stimulated HMF outgrowth, and there was no effect on the 3Y1-Ad12 control cells (Fig. 1Ba), suggesting that secreted catalytically-inactive pro-cath-D promotes 3D outgrowth of HMFs in a paracrine manner. Overall, our findings support the concept that pro-cath-D secreted by epithelial cancer cells might display a crucial paracrine effect on breast fibroblasts in a manner independent of its catalytic activity.

Cath-D interacts with the LRP1 receptor in vitro

Because cath-D hypersecreted by cancer cells is able to stimulate fibroblast outgrowth in a paracrine manner that is independent of its catalytic activity, we postulate that pro-cath-D secreted by cancer cells might act via its interaction with potential receptors present on the fibroblast cell surface. To identify possible cath-D partners, we performed a yeast two-hybrid screen using a LexA DNA-binding domain fused to 48-kDa intermediate cath-D as bait, and a cDNA library isolated from normal breast. The clone isolated in our screen was 100% identical to amino acids 307–479 of the extracellular domain of the LRP1 β chain (Fig. 2A).

To validate the cath-D–LRP1 interaction, we next performed GST pull-down experiments. The polypeptide containing amino acids 307–479 of the extracellular domain of the LRP1β chain, GST-LRP1β(307–479), was expressed as a GST-fusion protein, and tested for its ability to bind to pro-cath-D (Fig. 2B, left panel). Our results show that pro-cath-D bound to GST-LRP1β(307–479) (Fig. 2B, right panel). Subsequently, we performed GST pull-down experiments using GST-fusion proteins containing the 52-kDa pro-cath-D, 34-kDa cath-D heavy chain, 14-kDa cath-D light chain, or 4-kDa cath-D propeptide (Fig. 2C, left panels). The full-length extracellular LRP1β domain, LRP1β(1–476), was shown to bind effectively to 52-, 34- and 14-kDa cath-D fragments, but poorly to the 4-kDa cath-D propeptide (Fig. 2C, right panels), indicating that the interaction interface spans both the 34- and 14-kDa cath-D subunits.

The LRP1β(307–479) domain contains four juxtaposed complete EGF-like repeats (repeats 19–22) (Fig. 3Aa). In order to identify the LRP1β cath-D-binding domain, GST-fusion proteins containing various fragments of LRP1β(307–479) were tested for their ability to bind to pro-cath-D (Fig. 3Ab). We identified the F4 fragment of LRP1β(349–394), which contains the EGF-like repeat 20, as the shortest fragment able to bind pro-cath-D, when compared with F7 (307–348), F6 (394–432) or F8 (433–479) fragments of LRP1β (Fig. 3Ba). It is worth noting that LRP1β(307–479) also contains other important domains, because the F4 (349–394) fragment was partially active in pro-cath-D binding when compared with F0 (307–479). The abilities of smaller LRP1β fragments (F5, F9–F13) derived from F4, and of the F14 fragment covering the entire EGF-like repeat 20 (residues 360–396) to interact with pro-cath-D (Fig. 3B, top and bottom panels a and b) were both substantially impaired, suggesting that the intact F4 (349–394) fragment is required for the cath-D–LRP1β interaction. Because of the lack of disulfide linkage in *E. coli*, we verified that binding of pro-cath-D was comparable after

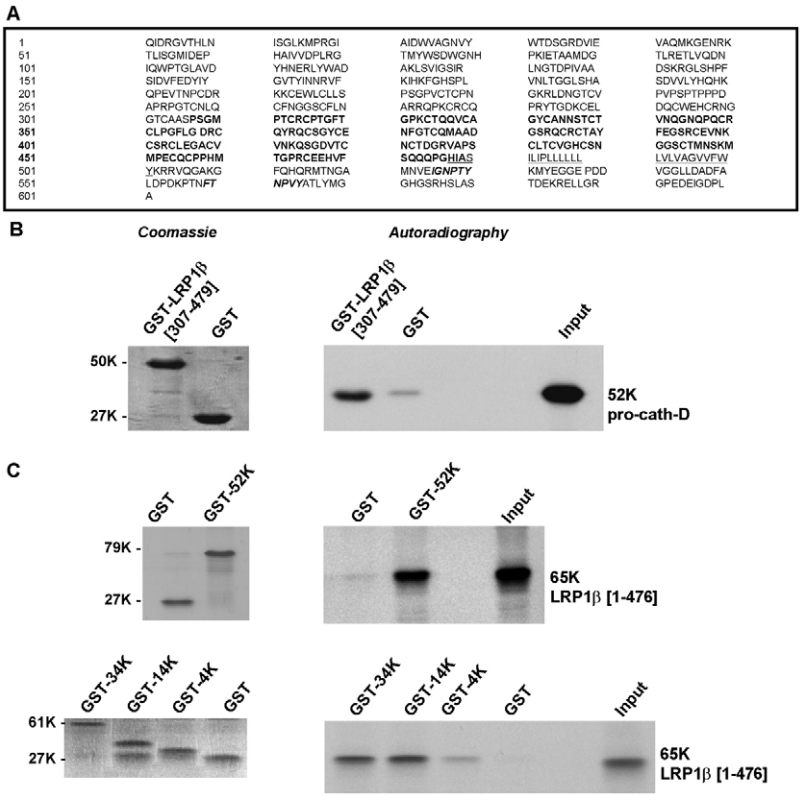

Fig. 2. Pro-cath-D interacts with the β chain of LRP1 in vitro. (**A**) Sequence of the LRP1 β chain, which interacts with cath-D, isolated by yeast two-hybrid. LRP1 is synthesized as a 4544-amino-acid precursor that is cleaved into an α chain and a β chain. The sequence of the β chain is shown, with the amino acids numbered starting at the first residue of the β chain. Residues 307–479, isolated by the yeast two-hybrid method, are shown in bold. The transmembrane sequence is underlined, and the two Asn-Pro-Xxx-Tyr (NP_XY) endocytosis motifs are in italics. (**B**) Binding of pro-cath-D to LRP1β(307–479) by GST pull-down. Radiolabeled pre-pro-cath-D proform synthesized from the reticulocyte lysate system was incubated with glutathione-Sepharose beads containing GST–LRP1β(307–479) or GST. GST proteins stained by Coomassie are shown in left panel. Bound pre-pro-cath-D was detected by autoradiography (right panel). (**C**) Binding of the full-length extracellular domain of LRP1β to pro-cath-D by GST pull-down. The radiolabeled, full-length extracellular domain of LRP1β(1–476) was incubated with beads containing GST fused to the 52-kDa form of cath-D (GST–cath-D/52K), GST–cath-D/34K, GST-cath-D/14K, GST-cath-D/4K or GST. GST proteins were stained by Coomassie (left panels). Bound LRP1β(1–476) was detected by autoradiography (right panels). The input (1/10) corresponds to the lysate used for the binding reaction. K, molecular mass in kilodaltons.

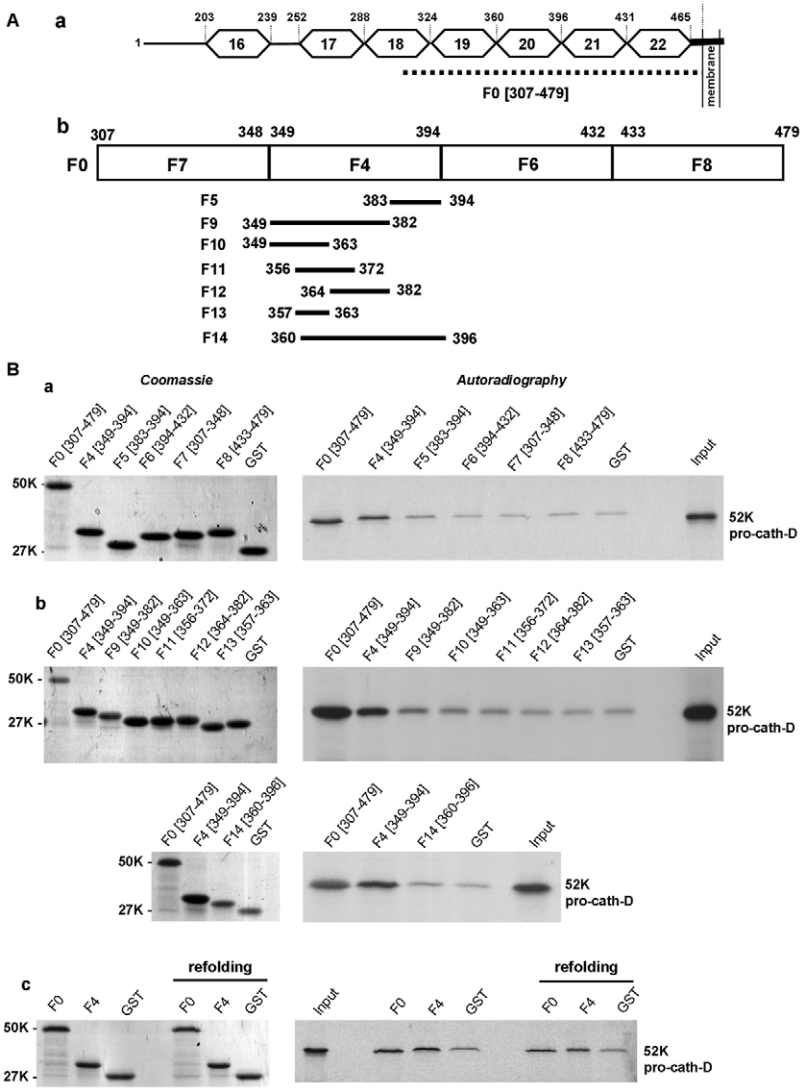

Fig. 3. Pro-cath-D binds to residues 349–394 of LRP1β in vitro. (**A**) Schematic representation of the LRP1β extracellular domain and GST–LRP1β fragments. A schematic representation of EGF-like repeats 16–22 located in the full-length extracellular domain of LRP1β is shown in panel a. The F0 (307–479) fragment, which interacts with cath-D, is indicated by a dotted line. GST–LRP1β fragments (F4, F6, F7 and F8) were derived from F0 (panel b). The F4 (349–394) GST-LRP1β fragment was then subdivided into seven fragments (F5, F9–F14) (panel b). (**B**) Binding of pro-cath-D to GST–LRP1β fragments. Radiolabeled pre-pro-cath-D was incubated with beads containing GST–LRP1β fragments or GST. GST proteins bound to beads were stained by Coomassie (left panels a-c), and bound pre-pro-cath-D was detected by autoradiography (right panels a-c). The binding of pre-pro-cath-D to the fragments derived from F0 is shown in panel a. The binding of pre-pro-cath-D to fragments derived from F4 is shown in panel b. The binding of pre-pro-cath-D after GST–F0 and GST–F4 refolding is shown in panel c. The input (1/10) corresponds to the lysate used for the binding reaction. K, molecular mass in kilodaltons.

GST-LRP1β F0 and F4 refolding (Fig. 3Bc). Our results provide independent confirmation of the yeast two-hybrid screen, and reveal direct interaction between cath-D and residues 349–394 of the extracellular domain of the LRP1 β chain.

Pro-cath-D partially colocalizes with LRP1 at the cell surface in transfected COS cells and in fibroblasts

We next investigated whether pro-cath-D colocalizes with LRP1β at the cell surface of intact cells. Non-permeabilized COS cells transiently co-transfected with pro-cath-D and Myc–LRP1β were analyzed by immunocytochemistry after double staining with a monoclonal antibody recognizing only the pro-cath-D proform, and a polyclonal antibody directed against the N-terminal Myc-tag of LRP1β. Fig. 4A shows that pro-cath-D (in red; panel b) partially colocalized (panel c) with LRP1β (in green; panel a) in punctuate structures. To confirm that secreted pro-cath-D colocalizes with LRP1 at the cell surface, cellular colocalization of LRP1 and pro-cath-D was further analyzed by immunogold electron microscopy in COS cells transiently co-transfected with pro-cath-D and LRP1β after double staining with an anti-pro-cath-D monoclonal antibody and a polyclonal antibody directed against the cytoplasmic tail of LRP1β (Fig. 4B). We observed colocalization of pro-cath-D and the LRP1β chain at the cell surface (Fig. 4B). Colocalization at the cell surface was also observed in COS cells transiently transfected with LRP1β and incubated with 15-nM pro-cath-D (data not shown). To investigate the interaction of secreted cath-D with endogenous LRP1, HMFs were incubated with 15 nM of pro-cath-D, and colocalization was analyzed by immunogold electron microscopy (Fig. 4C). Our data reveal that, in HMFs, pro-cath-D and LRP1β colocalize at the cell surface (Fig. 4C). Altogether, our findings indicate that, in intact cells, pro-cath-D and LRP1β colocalize at the cell surface.

Overexpressed LRP1β directs pro-cath-D to lipid rafts in transfected COS cells

A previous report described that LRP1 is localized both at the cell surface and in early endosomes (Herz and Strickland, 2001). Interestingly, some of the cell surface LRP1 is located in lipid rafts (Wu and Gonias, 2005; Zhang et al., 2004). Therefore, we next investigated whether pro-cath-D and LRP1 might colocalize at the cell surface in these micro-domains. COS cells transfected with cath-D (Fig. 5A) or co-transfected with pro-cath-D and LRP1β (Fig. 5B) were subjected to sucrose density ultracentrifugation. The raft markers flotillin and ganglioside GM1 were found

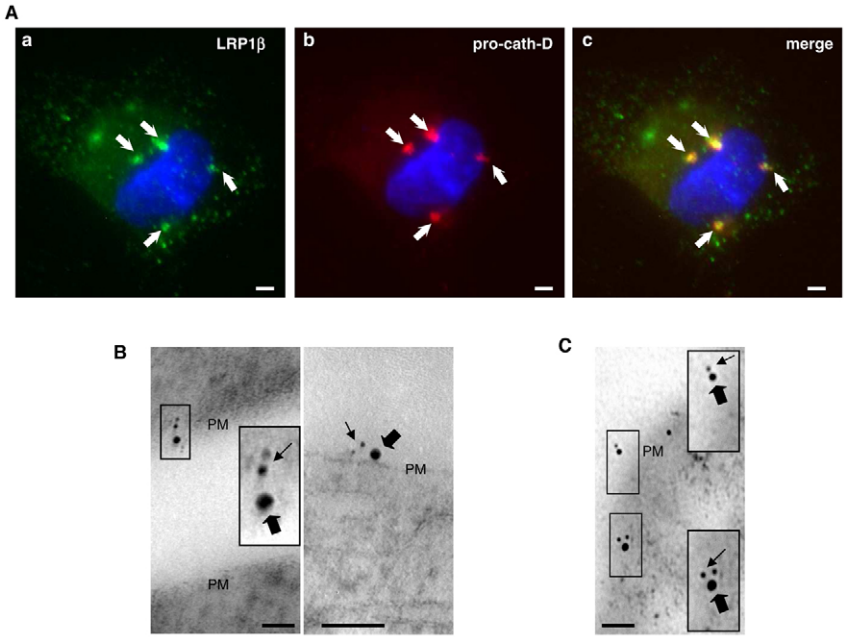

Fig. 4. Pro-cath-D and LRP1β partially colocalize at the cell surface in transfected COS cells and HMFs. (**A**) Co-transfected pro-cath-D and LRP1β colocalize partially in punctuate structures. Non-permeabilized COS cells transiently co-expressing cath-D and Myc–LRP1β were stained with a monoclonal anti-cath-D recognizing only the proform (red) and with a polyclonal anti-Myc-tagged LRP1β (green) antibody. DNA was visualized by incubation with 0.5 μg/ml cell-permeant Hoechst 33342 dye (blue). Panel a shows LRP1β staining. Panel b shows pro-cath-D staining. Panel c shows the double-staining pattern. Arrows indicate pro-cath-D and LRP1β colocalization. Scale bars: 15 μm. (**B**) Immunogold-labeled pro-cath-D and LRP1β colocalize at the cell surface in transfected COS cells. COS cells transiently co-expressing cath-D and Myc–LRP1β were double stained with a monoclonal anti-pro-cath-D antibody recognizing only the proform and conjugated to 6-nm gold particles (thin arrows), and with a polyclonal anti-LRP1β antibody conjugated to 15-nm gold particles (thick arrows). Left and right panels illustrate colocalization at the plasma membrane (PM). High magnifications of the boxed regions are displayed. Scale bars: 50 nm. (**C**) Immunogold-labeled pro-cath-D and LRP1β colocalize at the cell surface and in vesicular-like structures in HMFs. COS cells were transfected with cath-D, and 48 hours post-transfection conditioned medium containing 15 nM of pro-cath-D was added to HMF cells. HMFs incubated with pro-cath-D for 24 hours were double stained with a monoclonal anti-pro-cath-D antibody recognizing only the proform and conjugated to 6-nm gold particles (thin arrows), and with a polyclonal anti-LRP1β antibody conjugated with 15-nm gold particles (thick arrows). Panels illustrate colocalization at the plasma membrane (PM). High magnifications of the boxed regions are displayed. Scale bar: 50 nm.

predominantly in the low density fractions 4–6, whereas the non-raft marker, transferrin receptor (TfR), was found at the bottom of the sucrose gradient (Fig. 5, bottom panels). Endogenous LRP1β was detected in both the raft-rich and non-raft fractions (Fig. 5A, top). Pro-cath-D was mainly located in the non-raft fractions 7 and 8, although both pro-cath-D and its 48-kDa intermediate form were also detected in the raft-rich fractions 5 and 6 (Fig. 5A, middle). Interestingly, overexpression of LRP1β (Fig. 5B, top) resulted in a substantial increase of pro-cath-D in the raft-rich fractions (Fig. 5B, middle). These findings reveal, for the first time, the presence of pro-cath-D at the cell surface in lipid rafts, and strongly suggest that LRP1β enrichment in lipid rafts can direct pro-cath-D to these micro-domains.

Cath-D interacts with LRP1β in transfected COS cells and in fibroblasts

To find out whether pro-cath-D interacts with the LRP1β chain in cellulo, LRP1β was co-transfected into COS cells in the presence of wild-type pro-cath-D or of a pro-cath-D mutant devoid of proteolytic activity (^{D231N}cath-D). Unfortunately, no antibody recognizing only pro-cath-D was available for immunoprecipitation. We therefore used the anti-cath-D M1G8 antibody, which recognizes the 52-, 48- and 34-kDa forms of cath-D. This meant that immunoprecipitation with M1G8 would precipitate extracellular 52-kDa pro-cath-D associated with the cell surface, and intracellular 52-, 48- and 34-kDa forms of cath-D. Our results using anti-LRP1β antibody show that wild-type and D231N pro-cath-D were both coimmunoprecipitated with LRP1β (Fig. 6Aa, top). Longer gel exposure revealed that mature 34-kDa cath-D was also coimmunoprecipitated with LRP1β (Fig. 6Ab), suggesting that pro-cath-D and the associated LRP1 β chain can be directed to the lysosomes. Reciprocally, LRP1β was coimmunoprecipitated with cath-D or ^{D231N}cath-D using anti-cath-D M1G8 antibody (Fig. 6Aa, bottom). ^{D231N}cath-D displayed greater electrophoretic mobility, corresponding to an apparent molecular mass shift of ~1 kDa (Fig. 6Aa, top), as previously reported (Laurent-Matha et al., 2006). These findings demonstrate that the LRP1 β chain interacts preferentially with the 52-kDa pro-cath-D. We therefore conclude that co-transfected pro-cath-D and LRP1β interact in cellulo.

In order to study endogenous interaction in intact cells, we screened a variety of cell lines for LRP1 expression (supplementary material Fig. S1). Cath-D is known to be overexpressed and hypersecreted by breast cancer cells (Capony et al., 1989), but our survey revealed that breast cancer cells (MCF-7 and MDA-MB-231) express low levels of LRP1 (supplementary material Fig. S1). By contrast, LRP1 was highly expressed in all the fibroblastic cell lines tested: PEA10 (*LRP1*$^{+/-}$ MEF), *CD55*$^{-/-}$ cath-D (*cath-D*$^{-/-}$ MEFs transfected with human cath-D) and CCL146 mouse fibroblasts, and HMF and CCD45K human fibroblasts (supplementary material Fig. S1). However, as previously reported,

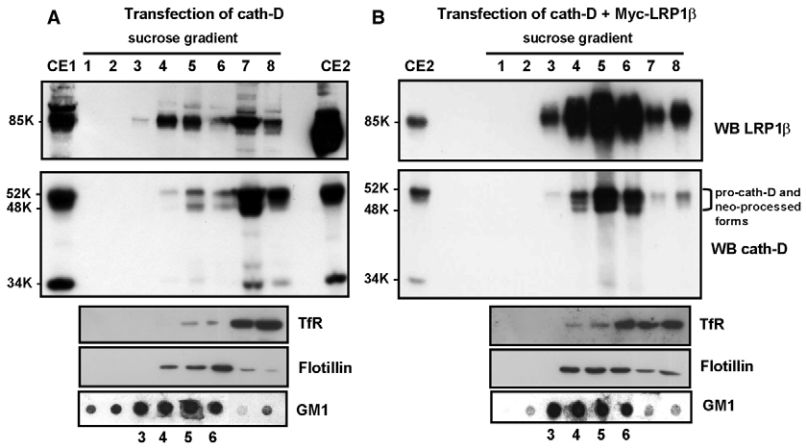

Fig. 5. LRP1β enhances pro-cath-D localization in rafts in transfected COS cells. COS cells transfected with cath-D (**A**) or cath-D + LRP1β (**B**) were unwashed and lysed 48 hours post-transfection. Lysates were submitted to sucrose density ultracentrifugation. Fractions were analyzed for anti-LRP1β (top panels) or anti-cath-D (middle panels) by immunoblotting. Cell lysates (100 μg) from cath-D-transfected (CE1) and cath-D + LRP1β-co-transfected COS cells (CE2) were analyzed by immunoblotting. CE2 was loaded onto both gels (A,B) as an internal control for cath-D or LRP1β enrichment relative to film exposure. Brackets indicate pro-cath-D and its neo-processed forms. Flotillin was used as a marker of raft fractions, and TfR as a marker of non-raft fractions (bottom panels). Each fraction was dot-blotted to detect ganglioside GM1 (bottom panels). K, molecular mass in kilodaltons.

fibroblasts do not secrete detectable levels of pro-cath-D (Laurent-Matha et al., 2005).

Because the cells that express high LRP1 levels and those that secrete pro-cath-D are distinct, we next studied the interaction of cath-D with endogenous LRP1β using *cath-D*$^{-/-}$ MEF cells stably transfected with human wild-type (*CD55*$^{-/-}$ cath-D) or mutated D231N cath-D (*CD55*$^{-/-}$ D231N) that had previously been shown to hypersecrete pro-cath-D (Laurent-Matha et al., 2005). Anti-cath-D M1G8 immuno-affinity purification revealed that LRP1β was co-eluted with both wild-type (Fig. 6Ba) and D231N cath-D (supplementary material Fig. S2). These results indicate that endogenous LRP1 interacts with stably transfected cath-D in fibroblasts.

We finally investigated the interaction of cath-D with endogenous LRP1β in HMFs incubated with 15 nM of pro-cath-D by immuno-affinity purification using M1G8 antibody. LRP1β was co-eluted with cath-D (Fig. 6Bb). We conclude that endogenous LRP1β interacts with cath-D in fibroblasts. Altogether, our data indicate that pro-cath-D interacts with LRP1β in cellulo.

Human cath-D requires LRP1 expression to trigger 3D outgrowth of fibroblasts

Because we had identified LRP1 as a fibroblastic receptor for pro-cath-D, we went on to check whether cath-D would induce fibroblast outgrowth via its interaction with LRP1.

To investigate the possible implication of LRP1 in the cath-D-induced fibroblast outgrowth, we performed 3D culture assays in cath-D-transfected fibroblasts hypersecreting pro-cath-D (*CD55*$^{-/-}$ cath-D) or mutated D231N pro-cath-D (*CD55*$^{-/-}$ D231N), which had or had not been silenced for LRP1 (Fig. 7Aa). As previously shown (Laurent-Matha et al., 2005), *cath-D*$^{-/-}$ MEF cells transfected with an empty vector (*CD55*$^{-/-}$ SV40) did not grow in Matrigel, and transfecting wild-type or mutated cath-D into *cath-D*$^{-/-}$ MEF cells led to a switch to fibroblast outgrowth (Fig. 7Ab), indicating cath-D-induced fibroblast outgrowth. We therefore analyzed the consequences of silencing LRP1 in these cells. The effect of LRP1 silencing on *CD55*$^{-/-}$ cath-D outgrowth was shown by phase-contrast microscopy (Fig. 7Ba, top) and by cell staining (Fig. 7Ba, bottom). Our findings indicate that LRP1 silencing in *CD55*$^{-/-}$ cath-D cells using *LRP1* siRNA3 (Fig. 7Bc) significantly reduced their cath-D-dependent outgrowth compared with cells transfected with *luc* siRNA (P<0.0125; Fig. 7Ba,Bb). Similar results were observed using *LRP1* siRNA4 (supplementary material Fig. S3). These findings indicate that cath-D requires LRP1 expression to promote fibroblast outgrowth. However, interestingly, LRP1 silencing in *CD55*$^{-/-}$ D231N cells also significantly inhibited their outgrowth, indicating the existence of a mechanism independent of cath-D proteolytic activity (P<0.0125; Fig. 7C).

To further investigate whether LRP1 mediates the paracrine action of secreted pro-cath-D on fibroblast outgrowth, we next performed 3D co-culture assays (Fig. 8A) with HMFs transfected with *luc* or *LRP1* siRNA (Fig. 8B) and co-cultured with 3Y1-Ad12 cancer cells secreting or not secreting wild-type or D231N cath-D (Fig. 8C). The co-culture assay revealed that only pro-cath-D-secreting 3Y1-Ad12 cells stimulated the outgrowth of HMFs transfected with *luc* siRNA, in contrast to 3Y1-Ad12 control cells (Fig. 8D). This outgrowth was shown by phase-contrast microscopy (Fig. 8D, top) and by cell staining (Fig. 8D, bottom). Our results further showed that silencing LRP1 in HMFs using siRNA1 (Fig. 8E) blocked their mitogenic response to secreted pro-cath-D as shown by phase-contrast microscopy (Fig. 8E, top) and by cell staining (Fig. 8E, bottom). Similar results were obtained with *LRP1* siRNA2 (supplementary material Fig. S4). In control experiments, we confirmed that the viability of HMF cells remained unaffected by LRP1 silencing. Phase-contrast microscopy showed that HMFs transfected with *luc* siRNA adopted an elongated morphology typical of fibroblasts [supplementary material Fig. S5a,b (see insets)]. LRP1 silencing using siRNA1 or siRNA2 analyzed by western blot (supplementary material Fig. S5a,b) induced a rounder shape and fewer protrusions when compared with *luc*-siRNA-transfected cells [supplementary material Fig. S5a,b (see insets)]. This suggests that LRP1 expression is required for the elongated fibroblast 3D morphology. The cell viability of HMF cells embedded in Matrigel was, however, not altered by LRP1 silencing. This was shown by cell staining in Matrigel (supplementary material Fig. S5a, bottom), and by cell cycle analyses using flow cytometry of cells extracted from Matrigel (proliferating cells in S and G2M phases=17% and 19.7% for *luc* siRNA and *LRP1* siRNA1 HMF cells, respectively). Altogether, these findings highlight that pro-cath-D secreted by epithelial cancer cells promotes fibroblast outgrowth in a paracrine, LRP1-dependent manner (Fig. 9).

Discussion

In this study, we identify the LRP1 receptor as a binding partner for pro-cath-D in fibroblasts. The cath-D–LRP1β interaction discovered by a yeast two-hybrid screen was further confirmed by GST pull-down, coimmunoprecipitation, co-purification and colocalization.

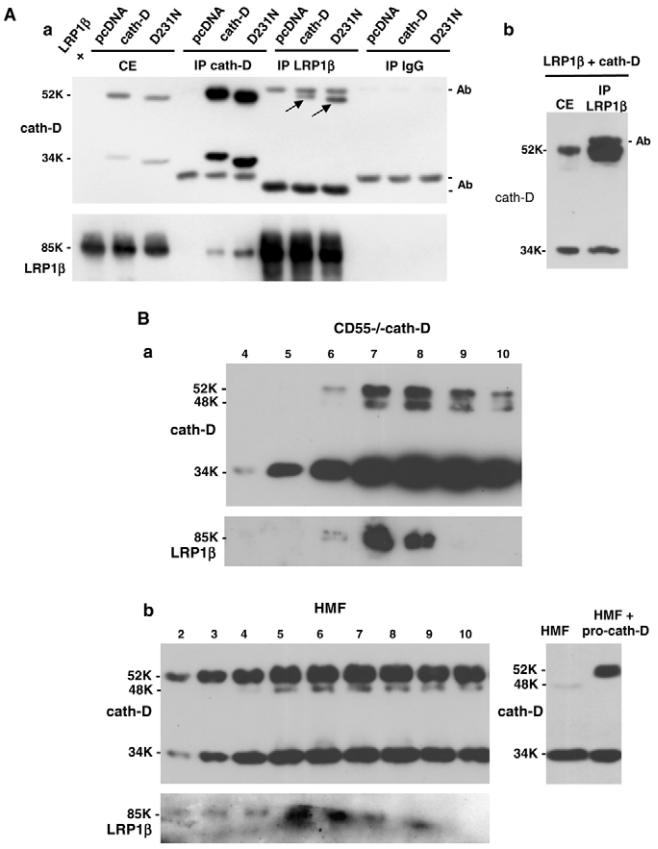

Fig. 6. Cath-D interacts with LRP1β in transfected COS cells and in fibroblasts. (**A**) Coimmunoprecipitation of co-transfected pro-cath-D and LRP1β in COS cells. COS cells were transiently co-transfected with LRP1β expression vector, and pcDNA, cath-D or ^{D231N}cath-D vectors. At 48 hours post-transfection, unwashed cells were lysed in PLC buffer. Cell extracts (CE), and cath-D, LRP1β and non-immune IgG immunoprecipitations (IP) performed with anti-LRP1β 11H4 hybridoma or anti-cath-D M1G8 antibody were analyzed by anti-cath-D (panel a, top) and anti-LRP1β (panel a, bottom) immunoblotting. Arrows show coimmunoprecipitated pro-cath-D. A longer gel exposure of the LRP1β immunoprecipitation performed in COS cells co-transfected with LRP1β and cath-D vectors and analyzed by anti-cath-D immunoblotting is shown in panel b. (**B**) Co-purification of endogenous LRP1 with cath-D in fibroblasts. Co-purification of endogenous LRP1 with cath-D in cath-D-transfected MEFs (*CD55*$^{-/-}$cath-D) (panel a). Cells grown to 90% confluence without medium change for 3 days were directly lysed in PLC buffer, and loaded on an anti-cath-D M1G8 affinity column that binds to 52-, 48- and 34-kDa forms of cath-D. Eluted fractions were subjected to SDS-PAGE and immunoblotted with the anti-cath-D antibody (top panel) and anti-LRP1β hybridoma (bottom panel). Co-purification of endogenous LRP1 with cath-D in HMF cells treated with pro-cath-D (panel b, left). COS cells were transfected with cath-D, and 48 hours post-transfection conditioned medium containing 15 nM of pro-cath-D was added to HMF cells. Unwashed HMFs incubated for 48 hours with conditioned medium containing 15 nM of pro-cath-D were directly lysed in PLC buffer. HMF cell extracts were purified on the M1G8-coupled column and analyzed by immunoblotting as described in A. Detection of cath-D in a HMF lysate incubated with or without the conditioned medium containing pro-cath-D is shown in panel b (right). K, molecular mass in kilodaltons.

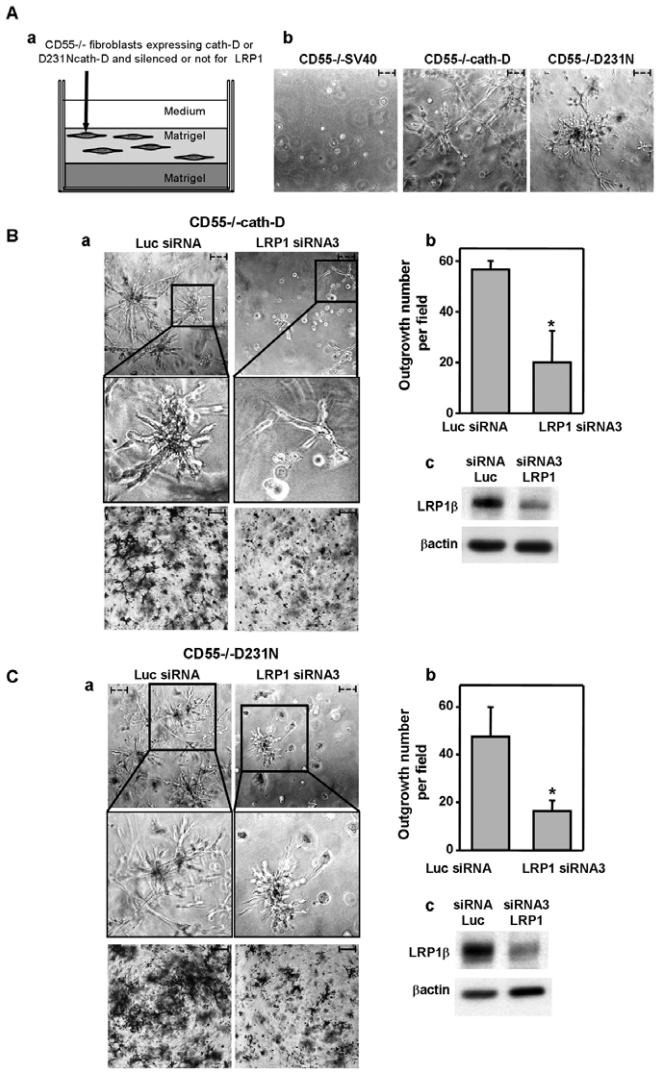

Fig. 7. Silencing LRP1 inhibits the outgrowth capacities of cath-D- and ^{D231N}cath-D-secreting MEFs. (**A**) Matrigel outgrowth of cath-D-transfected MEFs. *CD55*$^{-/-}$SV40, *CD55*$^{-/-}$cath-D and *CD55*$^{-/-}$D231N fibroblasts were embedded in Matrigel (panel a). Phase-contrast optical photomicrographs of *CD55*$^{-/-}$SV40, *CD55*$^{-/-}$cath-D and *CD55*$^{-/-}$D231N fibroblasts are shown after culturing for 3 days (panel b). (**B**) Silencing LRP1 in pro-cath-D-secreting MEFs inhibits outgrowth. *CD55*$^{-/-}$cath-D cells transfected with *LRP1* siRNA3 or *luc* siRNA were embedded in Matrigel 24 hours post-transfection (panel a). Phase-contrast optical photomicrographs (panel a, top), and p-nitrotetrazolium violet cell staining (panel a, bottom) are shown after culturing for 3 days. High magnifications of the boxed regions are displayed. For quantification, the number of outgrowth with protruding fibroblasts as detected with the p-nitrotetrazolium violet were counted by two independent investigators (double blind) in three low-magnification fields (panel b). *P<0.0125; Student's t-test. LRP1β expression was monitored 24 hours post-transfection of *CD55*$^{-/-}$cath-D cells with *luc* siRNA or *LRP1* siRNA3 (panel c). Scale bars: broken line, 75 μm; solid line, 750 μm. Data from one representative experiment out of three are shown. (**C**) Silencing LRP1 in pro-^{D231N}cath-D-secreting MEFs inhibits outgrowth. *CD55*$^{-/-}$D231N fibroblasts transfected with *LRP1* siRNA3 or *luc* siRNA were embedded in Matrigel 24 hours post-transfection and analyzed as described in B. *P<0.0125; Student's t-test.

Our results demonstrate that, in fibroblasts, the pro-cath-D protease interacts with the extracellular domain of the β chain of LRP1, and establishes pro-cath-D as the first ligand of the extracellular LRP1 β chain to be identified. We identified the F4 LRP1β(349–394) fragment, which contains the EGF-like repeat 20 with an additional 11 amino acids at its N-terminus, as the shortest fragment able to bind pro-cath-D. No ligand has previously been described as binding

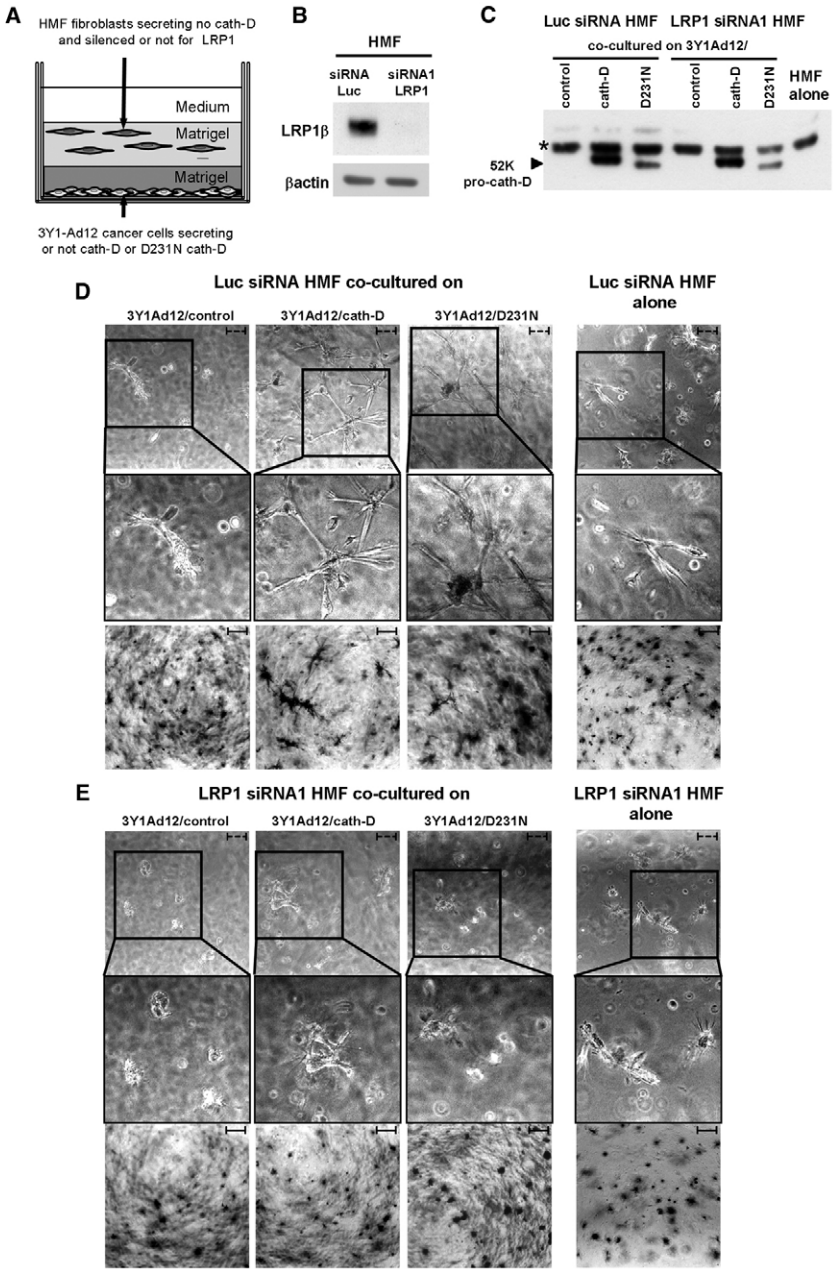

Fig. 8. Silencing LRP1 in HMFs inhibits the paracrine stimulation of fibroblast outgrowth induced by secreted pro-cath-D. HMFs transfected with *luc* siRNA or *LRP1* siRNA1 were embedded 48 hours post-transfection in the presence of a bottom layer of 3Y1-Ad12 cancer cell lines secreting or not pro-cath-D or D231N pro-cath-D (**A**). LRP1β expression was monitored 48 hours post-transfection and before the co-culture assays (**B**). Pro-cath-D secretion was analyzed by immunoblotting after co-culturing for 3 days with *luc*-siRNA- or *LRP1*-siRNA1-transfected HMFs, with 3Y1-Ad12 control or cath-D-transfected cells (**C**). *Non-specific contaminant protein. Phase-contrast optical photomicrographs (**D**, top), and p-nitrotetrazolium violet cell staining (D, bottom) are shown after culturing for 3 days with HMFs transfected with *luc* siRNA. Phase-contrast optical photomicrographs (**E**, top) and p-nitrotetrazolium violet cell staining (E, bottom) are shown after culturing for 3 days with HMFs transfected with *LRP1* siRNA1. High magnifications of the boxed regions are displayed. Data from one representative experiment out of three is shown. Broken line, 75 μm; solid line, 750 μm.

to this particular region, and the biological relevance of the EGF-like repeats in the extracellular domain of LRP1β is still unknown. Our results reveal that pro-cath-D colocalized with LRP1β at the cell surface in lipid rafts. At the cell surface, LRP1 has been shown to be localized in clathrin-coated pits and in lipid rafts (Boucher et al., 2002; Wu and Gonias, 2005; Zhang et al., 2004). Here, we show that LRP1β overexpression directs pro-cath-D to the lipid rafts. Interestingly, this study reveals, for the first time, the presence of pro-cath-D in lipid rafts. The lysosomal cysteine protease cathepsin B (cath-B) is also known to localize within these lipid micro-domains in association with the annexin II heterotetramer (Mohamed and Sloane, 2006). A previous study excluded LRP1 as a possible cath-D receptor (Laurent-Matha et al., 2002). These observations were based on the use of the RAP chaperone protein (Herz, 2006), which competes with ligands that bind to the LRP1 α chain (Laurent-Matha et al., 2002). We checked that RAP protein did not bind to LRP1β, and that the pro-cath-D–LRP1β interaction was not abolished by RAP (data not shown). Consequently, our finding that cath-D binds to the LRP1 β chain explains why RAP did not compete with cath-D for binding to LRP1.

Cancer is a tissue-based disease in which malignant cells interact dynamically with many normal cell types, such as fibroblasts (Mueller and Fusenig, 2004). The fibroblast is a major cell type of the stromal compartment, and is intimately involved in orchestrating the stromal part of the dialogue in tissue homeostasis (Grinnell, 1994; Elenbaas et al., 2001). A stromal reaction immediately adjacent to transformed epithelial cells has been documented in several tumor systems (Basset et al., 1990). Whereas the role of matrix metalloproteinases and urokinase plasminogen activator in the stromal compartment has been documented in various studies (Liotta and Kohn, 2001), the potential role of cath-D in fibroblasts has not yet been fully determined. It has been proposed that cath-D that is

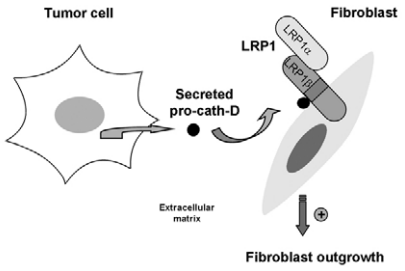

Fig. 9. Model of cath-D paracrine action through the LRP1 receptor. We propose that pro-cath-D hypersecreted by cancer cells stimulates fibroblast outgrowth in a paracrine LRP1-dependent manner.

localized at the surface of breast fibroblasts might be mitogenic (Koblinski et al., 2002), or that intracellular cath-D in fibroblasts might assist cancer cells to digest the extracellular matrix during tissue invasion (Heylen et al., 2002). We had previously observed that pro-cath-D secreted by cancer cells mediates mouse embryonic fibroblast outgrowth in a paracrine manner (Laurent-Matha et al., 2005), suggesting its key role in the tumor microenvironment. In the present study, we validate these findings in HMFs, indicating the relevance of the paracrine role of secreted pro-cath-D in the tumor microenvironment in the pathological context. We also demonstrate that LRP1 is the fibroblastic receptor responsible for stimulating the pro-cath-D-induced outgrowth. Our 3D co-culture outgrowth assays with cancer cells, which did or did not secrete human pro-cath-D, and HMFs, which had or had not been silenced for LRP1, reveal that pro-cath-D requires LRP1 expression to promote HMF outgrowth. These data support a model in which pro-cath-D hypersecreted by cancer cells stimulates the outgrowth of surrounding fibroblasts in a paracrine and LRP1-dependent manner in the breast tumor microenvironment. It is worth noting that LRP1 might be involved in the onset and progression of various human malignancies, because LRP1 is expressed by fibroblasts in breast cancer biopsies, and also at the invasive front in colon cancer biopsies (Christensen et al., 1996; Obermeyer et al., 2007). In addition, C766T *LRP1* gene polymorphism is associated with an increased risk of breast cancer development (Benes et al., 2003). Moreover, recent studies have reported a stimulatory role of LRP1 in cancer cell proliferation, motility and invasion (Dedieu et al., 2008; Li et al., 2003; Song et al., 2009). Although breast cancer cells express LRP1 at a much lower level than do fibroblasts, several studies have reported that hypoxia upregulates LRP1 expression in breast cancer cells (Bando et al., 2003; Koong et al., 2000; Montel et al., 2007). It is therefore possible that cath-D-enhanced breast cancer cell proliferation might be also dependent on LRP1 expression, acting via an autocrine loop. Our outgrowth assays using cells hypersecreting pro-cath-D or not, and silenced for LRP1 or not, strongly suggest that cath-D also promotes outgrowth via LRP1 in an autocrine manner. Future studies will investigate the possible relevance of the autocrine function of cath-D via LRP1 in breast cancer cells.

The mechanism by which LRP1 controls the cath-D-dependent stimulation of fibroblast outgrowth implies that cath-D has an action independent of its catalytic activity. The serine protease tPA has also been shown to act independently of its proteolytic activity as a cytokine via LRP1 (Hu et al., 2006). LRP1 is known to modify the extracellular microenvironment by internalizing numerous ligands via its α chain (Herz and Strickland, 2001), to control signal transduction pathways via cytoplasmic LRP1β tyrosine phosphorylation (Barnes et al., 2003; Boucher and Gotthardt, 2004; Boucher et al., 2002; Hu et al., 2006; Yang et al., 2004), and to modulate gene transcription by regulated intramembrane proteolysis (RIP) of its β chain (Kinoshita et al., 2003; May et al., 2002; von Arnim et al., 2005; Zurhove et al., 2008). Future research will investigate whether the pro-cath-D–LRP1β complex is internalized, and whether the pro-cath-D–LRP1β interaction can affect LRP1β tyrosine phosphorylation or LRP1β RIP.

In conclusion, we report, for the first time, that pro-cath-D interacts with the extracellular domain of the LRP1 β chain at the surface of fibroblasts, and that it promotes an LRP1-dependent fibroblast outgrowth independently of its catalytic activity. We propose that pro-cath-D, which is hypersecreted by breast cancer cells, might be involved in creating the tumor microenvironment that can sustain breast tumor growth and progression through its interaction with LRP1.

Materials and Methods

Materials

HMFs, kindly provided by Jacques Piette (IGM, Montpellier, France), were obtained from reduction mammoplasty tissues from a patient without cancer. Cath-D-deficient *CD55*$^{-/-}$ immortalized mouse fibroblasts transfected with empty vector (*CD55*$^{-/-}$ SV40), human cath-D (*CD55*$^{-/-}$ cath-D) or D231N mutated cath-D (*CD55*$^{-/-}$ D231N) were previously described (Laurent-Matha et al., 2005). 3Y1-Ad12 rat cancer cells transfected with empty vector (3Y1-Ad12/control), human cath-D (3Y1-Ad12/cath-D) or D231N mutated cath-D (3Y1-Ad12/D231N) were previously described (Glondu et al., 2001). PEA13 (*LRP1*$^{-/-}$ MEF) and PEA10 (*LRP1*$^{+/-}$ MEF) were purchased from the American Type Culture Collection (ATCC). Cells were cultured in DMEM with 10% fetal calf serum (FCS, GibcoBRL). The 11H4 hybridoma directed against the C-terminal intracellular part of the LRP1 β chain was purchased from ATCC. Polyclonal anti-human LRP1 β-chain antiserum directed against the C-terminal intracellular part of LRP1 β chain was previously described (Zhang et al., 2004). The anti-human, cath-D monoclonal antibody M2E8, used for immunofluorescence, interacts only with 52-kDa pro-cath-D, and not with 48- or 34-kDa cath-D (Freiss et al., 1988). The anti-human cath-D monoclonal antibody (BD Biosciences) used for immunoblotting recognized the 52-, 48- and 34-kDa forms of cath-D. The anti-human cath-D M1G8 monoclonal antibody used for immunoprecipitation and immunoaffinity purification recognized the 52-, 48- and 34-kDa forms of cath-D (Garcia et al., 1985). Control IgG1 MOPC-21 monoclonal antibody was purchased from Abcam, anti-β actin polyclonal antibody from Sigma, anti-human flotillin-1 monoclonal antibody from BD Biosciences, and anti-human transferrin receptor monoclonal antibody from Zymed. Pro-cath-D content of culture supernatants was determined by using a cath-D immunoradiometric assay (Garcia et al., 1985).

Plasmids

pcDNA3.1(+) Myc-tagged LRP1 β chain (Barnes et al., 2003), pcDNA3.1(–) cath-D and pcDNA3.1(–) ^{D231N}cath-D expression plasmids (Glondu et al., 2001) have previously been described. The pcDNA3.1(+) LRP1β extracellular domain (1–476) expression plasmid was created by inserting the PCR-amplified cDNA encoding LRP1β(1–476) from pcDNA3.1(+) Myc-tagged LRP1β into pcDNA3.1(+) previously digested by *Nhe*I and *Xba*I. pGEX-4T-1 LRP1β(307–479) was generated by inserting PCR-amplified cDNA encoding LRP1β(307–479) from pYESTrp2–LRP1β(307–479) identified by a two-yeast hybrid assay into pGEX-4T-1 previously digested by *Eco*RI. GEX-4T-1 LRP1β smaller fragments were generated by inserting PCR-amplified cDNA LRP1β shorter fragments from pYESTrp2–LRP1β(307–479) into pGEX-4T-1 previously digested by *Eco*RI and XhoI. Supplementary material Table S1 shows the primers used for LRP1β cloning. pGEX-2TK–cath-D constructs were obtained by inserting PCR-amplified cDNA encoding human 52-kDa pro-cath-D, 34-kDa and 14-kDa cath-D chains, and 4-kDa cath-D pro-fragment into pGEX-4T-1 previously digested by *Eco*RI. Supplementary material Table S1 shows the primers used for cath-D cloning.

Yeast two-hybrid assay

Human cath-D (48-kDa intermediate form) was fused with the LexA DNA-binding domain in the pMW101 vector. A cDNA library derived from normal breast tissue was cloned into the galactosidase-inducible pYESTrp2 vector (Invitrogen) containing a B42 activating domain. The yeast two-hybrid screen was performed as described previously (Slentz-Kesler et al., 2000).

siRNA transfections and outgrowth assays

Approximately 30,000 HMF cells were transiently transfected with 10 μg human *LRP1* or *luc* siRNAs using Oligofectamine (Invitrogen). Approximately 50,000 *CD55*$^{-/-}$ cath-D or *CD55*$^{-/-}$ D231N cells were transiently transfected with 2.5 μg mouse *LRP1* or *luc* siRNAs. Around 15,000 MCF-7 cells were transiently transfected with 1 μg siRNA using Oligofectamine (Invitrogen). For outgrowth assays, 50,000

CD55$^{-/-}$ cath-D or *CD55*$^{-/-}$ D231N cells were re-suspended at 4°C in Matrigel (BD Biosciences) 24 hours post-transfection with *LRP1* or *luc* siRNAs, and added to a pre-set layer of Matrigel (Glondu et al., 2001). In co-culture outgrowth assays, 15,000 MCF-7 cells previously transfected with *cath-D* or *luc* siRNAs, or 100,000 cells from control-, D231N- or cath-D-transfected 3Y1-Ad12 cell lines were plated and then covered first with a layer of Matrigel, and then with a layer of Matrigel containing 50,000 HMFs 48 hours post-transfection with *LRP1* or *luc* siRNAs (Laurent-Matha et al., 2005).

siRNAs

Duplexes of 21-nucleotide human *LRP1* siRNA1 (target sequence 5′-AAGCAGTTTGCCTGCAGAGAT-3′, residues 666–684) (Li et al., 2003), human *LRP1* siRNA2 (target sequence 5′-AAGCTATGAGTTTAAGAAGTT-3′) (Dharmacon), mouse *LRP1* siRNA3 (target sequence 5′-AAGCAUCUCA-GUAGACUAUCA-3′) (Fears et al., 2005), mouse *LRP1* siRNA4 (target sequence 5′-AAGCAGTTTGCCTGCAGAGAC-3′), human *cath-D* siRNA (target sequence 5′-AAGCUGGUGGACCAGAACAUC-3′, residues 666-684) (Bidere et al., 2003) or firefly luciferase (*luc*) siRNA (target sequence 5′-AACGTACGCGGAA-TACTTCGA-3′) were synthesized by MWG Biotech S.A. (France) or Dharmacon. Supplementary material Table S1 shows siRNA oligonucleotides.

GST pull-down assays

[^{35}S]methionine-labeled pre-pro-cath-D, and LRP1β (1-476) were obtained by transcription and translation using the TNT^{T7}-coupled reticulocyte lysate system (Promega). GST, GST-LRP1β fragments and GST–cath-D fusion proteins were produced in *Escherichia coli* B strain BL21 using isopropyl-1-thio-β-D-galactopyranoside (1 mM) for 3 hours at 37°C. GST-fusion proteins were purified on glutathione-Sepharose beads (Amersham Biosciences). For pull-down assays, 20 µl of glutathione-Sepharose beads with immobilized GST fusion proteins were incubated overnight at 4°C with [^{35}S]methionine-labeled proteins in 500 µl PDB buffer (20 mM HEPES-KOH, pH 7.9, 10% glycerol, 100 mM KCl, 5 mM $MgCl_2$, 0.2 mM EDTA, 1 mM DTT, 0.2 mM phenylmethylsulfonyl fluoride) containing 15 mg/ml BSA and 0.1% Tween 20. The beads were washed with 500 µl PDB buffer, and bound proteins were resolved by 15% SDS-PAGE, stained with Coomassie Blue, and exposed to autoradiographic film. The refolding of GST proteins was performed using a multi-step dialysis protocol (Protein refolding kit, Novagen) followed by disulfide-bond formation using a redox system (cysteine/cystine).

Co-transfection, coimmunoprecipitation and co-purification

COS cells were co-transfected with 10 µg of pcDNA3–Myc–LRP1β, and 10 µg of pcDNA3.1, pcDNA3.1–cath-D or pcDNA3.1–^{D231N}cath-D vectors. Transient transfection was carried out using Lipofectamine and Opti-MEM (Gibco-BRL). At 2 days post-transfection, cells were directly lysed in 50 mM HEPES (pH 7.5), 150 mM NaCl, 10% glycerol, 1% Triton X-100, 1.5 mM $MgCl_2$, 1 mM EGTA, 100 mM NaF, 10 mM sodium pyrophosphate, 500 µM sodium vanadate and a protease inhibitor cocktail (PLC lysis buffer). Lysates were incubated with 3 µg of anti-cath-D M1G8, or control IgG1 MOPC-21 monoclonal antibodies, or 40 µl of the anti-LRP1β 11H4 hybridoma overnight at 4°C, and subsequently with 25 µl of 10% protein G-Sepharose, for 2 hours at 4°C on a shaker. Sepharose beads were washed four times with PLC buffer, boiled for 3 minutes in SDS sample buffer, and resolved by SDS-PAGE and immunoblotting. For cath-D purification, unwashed cells were lysed in PLC buffer and were passed over an anti-cath-D M1G8-coupled agarose column. The column was washed with phosphate buffer (0.5 M $NaPO_4$, 150 mM NaCl, 0.01% Tween 80, 5 mM β-glycerophosphate) containing protease inhibitors, and then eluted in different fractions with 20 mM lysine, pH 11.

Isolation of lipid rafts

COS cells transfected as described above were lysed in MEB buffer (150 mM NaCl, 20 mM morpholine ethane sulfonic acid, pH 6.5) containing 1% Triton X-100, 1 mM Na_3VO_4, 50 mM NaF and protease inhibitor cocktail, and were homogenized using a Dounce homogenizer. The preparation was mixed with an equal volume of 80% sucrose solution in MEB buffer in an ultracentrifuge tube over-laid with 30% sucrose and 1.5 ml of 5% sucrose, and centrifuged at 39,000 rpm for 16 hours at 4°C in a Beckman SW40 Ti. After centrifuging, fractions were collected and subjected to immunoblot analysis. The ganglioside GM1 was detected with biotin-conjugated cholera toxin B subunit (Sigma-Aldrich) followed by incubation with horseradish-peroxidase-conjugated streptavidin and revealed by chemiluminescence (ECL, GE Healthcare).

Immunoblotting

Cell extracts (100 µg) or conditioned media (80 µl) were submitted to SDS-PAGE and anti-LRP1β, anti-cath-D or anti-β-actin immunoblotting.

Immunocytochemistry

Cells co-transfected with pro-cath-D and Myc-LRP1β were fixed with 4% paraformaldehyde and blocked with 2.5% goat serum (Sigma). Cells were incubated with the A-14 rabbit polyclonal antibody (10 µg/ml, Santa Cruz) recognizing the 9E10 Myc tag followed by an Alexa-Fluor-488-conjugated goat anti-rabbit IgG (1/200; Invitrogen). After washing, cells were incubated with an anti-pro-cath-D M2E8 mouse monoclonal (40 µg/ml) followed by an Alexa-Fluor-568-conjugated goat anti-mouse IgG (1/200; Invitrogen). DNA was visualized by incubation with 0.5 µg/ml cell-permeant Hoechst 33342 dye (Molecular Probes; 10 minutes). Microscopy slides were observed with a motorized Leica Microsystems (Rueil-Malmaison, France) DMRA2 microscope equipped with an oil immersion 100×/1.4 apochromatic objective and a 12-bit CoolSNAP FX CCD camera (Princeton Instruments, Roper Scientific, Evry, France), both controlled by the MetaMorph imaging software (Universal Imaging, Roper Scientific).

Immunogold

Cells grown in 24-well inserts were fixed with 3% paraformaldehyde and 0.1% glutaraldehyde in a phosphate buffer (pH 7.2) overnight at 4°C. Cells were cryoprotected with sucrose 3.5%, and stained for 2 hours with uranyl acetate 2% in a maleate buffer 0.05 M (pH 6.2) at room temperature. Cells were embedded in Lowicryl HM20 in a Leica EM AFS using the Progressive Lowering of Temperature method. Ultra-thin sections (85 nm) were first pre-incubated in PBS with 0.1% cold water fish gelatin, 1% BSA and 0.05% Tween 20 (incubation buffer) for 2 hours at room temperature, and then incubated with rabbit anti-LRP1β (1/20) and mouse anti-cath-D M2E8 (40 µg/ml) in the incubation buffer overnight at 4°C, and subsequently with 15 nm goat anti-rabbit-gold and 6-nm goat anti-mouse-gold 5 (Aurion) diluted 1/20 in the incubation buffer for 2 hours at 4°C. Sections were observed under a Hitachi 7100 transmission electron microscope.

Flow cytometry

Cells embedded in Matrigel were recovered after 3 days with 2.5 ml Matrisperse (Becton Dickinson), re-suspended in 1 ml of a solution containing 0.1% tri-sodium citrate dehydrate, 0.1% Triton X-100, 25 µg/ml propidium iodide and 100 µg/ml RNAse, prior to FACScan analysis (Becton Dickinson, CA) with an argon ion laser turned at 488 nm, 20 mW. Propidium iodide fluorescence was measured at 585 nm. Data were collected and analyzed with Cellquest (Becton Dickinson, CA) and ModFit (Verity Software, ME) software, respectively.

RNA extraction, RT-PCR and Q-PCR

RNA extraction and reverse transcription were performed, and quantitative PCR (Q-PCR) was carried out using a LightCycler and the DNA-double-strand-specific SYBR Green I dye for detection (Roche). Q-PCR was performed using gene-specific oligonucleotides, and results were normalized to RS9 levels.

We thank Nadia Kerdjadj for secretarial assistance, Jean-Yves Cance for the photographs and Chantal Cazevieille (Centre de Ressources en Imagerie Cellulaire, Montpellier) for the immunogold microscopy. We also thank Stephan Jalaguier for helpful discussions regarding the GST pull-down experiments. This work was supported by the 'Institut National de la Santé et de la Recherche Médicale', University of Montpellier I, 'ANR Jeunes Chercheuses, Jeunes Chercheurs' and the 'Ligue Nationale contre le Cancer', and the 'Association pour la Recherche sur le Cancer', which provided a fellowship for Mélanie Beaujouin.

Supplementary material available online at
http://jcs.biologists.org/cgi/content/full/123/19/3336/DC1

References

Bando, H., Toi, M., Kitada, K. and Koike, M. (2003). Genes commonly upregulated by hypoxia in human breast cancer cells MCF-7 and MDA-MB-231. *Biomed. Pharmacother.* **57**, 333-340.

Barnes, H., Ackermann, E. J. and van der Geer, P. (2003). v-Src induces Shc binding to tyrosine 63 in the cytoplasmic domain of the LDL receptor-related protein 1. *Oncogene* **22**, 3589-3597.

Basset, P., Bellocq, J. P., Wolf, C., Stoll, I., Hutin, P., Limacher, J. M., Podhajcer, O. L., Chenard, M. P., Rio, M. C. and Chambon, P. (1990). A novel metalloproteinase gene specifically expressed in stromal cells of breast carcinomas. *Nature* **348**, 699-704.

Benes, P., Jurajda, M., Zaloudik, J., Izakovicova-Holla, L. and Vacha, J. (2003). C766T low-density lipoprotein receptor-related protein 1 (LRP1) gene polymorphism and susceptibility to breast cancer. *Breast Cancer Res.* **5**, R77-R81.

Berchem, G., Glondu, M., Gleizes, M., Brouillet, J. P., Vignon, F., Garcia, M. and Liaudet-Coopman, E. (2002). Cathepsin-D affects multiple tumor progression steps in vivo: proliferation, angiogenesis and apoptosis. *Oncogene* **21**, 5951-5955.

Bidere, N., Lorenzo, H. K., Carmona, S., Laforge, M., Harper, F., Dumont, C. and Senik, A. (2003). Cathepsin D triggers Bax activation, resulting in selective apoptosis-inducing factor (AIF) relocation in T lymphocytes entering the early commitment phase to apoptosis. *J. Biol. Chem.* **278**, 31401-31411.

Boucher, P. and Gotthardt, M. (2004). LRP and PDGF signaling: a pathway to atherosclerosis. *Trends Cardiovasc. Med.* **14**, 55-60.

Boucher, P., Liu, P., Gotthardt, M., Hiesberger, T., Anderson, R. G. and Herz, J. (2002). Platelet-derived growth factor mediates tyrosine phosphorylation of the cytoplasmic domain of the low Density lipoprotein receptor-related protein in caveolae. *J. Biol. Chem.* **277**, 15507-15513.

Capony, F., Rougeot, C., Montcourrier, P., Cavailles, V., Salazar, G. and Rochefort, H. (1989). Increased secretion, altered processing, and glycosylation of pro-cathepsin D in human mammary cancer cells. *Cancer Res.* **49**, 3904-3909.

Capony, F., Braulke, T., Rougeot, C., Roux, S., Montcourrier, P. and Rochefort, H. (1994). Specific mannose-6-phosphate receptor-independent sorting of pro-cathepsin D in breast cancer cells. *Exp. Cell Res.* **215**, 154-163.

Christensen, L., Wiborg Simonsen, A. C., Heegaard, C. W., Moestrup, S. K., Andersen, J. A. and Andreasen, P. A. (1996). Immunohistochemical localization of urokinase-type plasminogen activator, type-1 plasminogen-activator inhibitor, urokinase receptor and alpha(2)-macroglobulin receptor in human breast carcinomas. *Int. J. Cancer* **66**, 441-452.

Dedieu, S., Langlois, B., Devy, J., Sid, B., Henriet, P., Sartelet, H., Bellon, G., Emonard, H. and Martiny, L. (2008). LRP-1 silencing prevents malignant cell invasion despite increased pericellular proteolytic activities. *Mol. Cell. Biol.* **28**, 2980-2995.

Elenbaas, B., Spirio, L., Koerner, F., Fleming, M. D., Zimonjic, D. B., Donaher, J. L., Popescu, N. C., Hahn, W. C. and Weinberg, R. A. (2001). Human breast cancer cells generated by oncogenic transformation of primary mammary epithelial cells. *Genes Dev.* **15**, 50-65.

Fears, C. Y., Grammer, J. R., Stewart, J. E., Jr, Annis, D. S., Mosher, D. F., Bornstein, P. and Gladson, C. L. (2005). Low-density lipoprotein receptor-related protein contributes to the antiangiogenic activity of thrombospondin-2 in a murine glioma model. *Cancer Res.* **65**, 9338-9346.

Ferrandina, G., Scambia, G., Bardelli, F., Benedetti Panici, P., Mancuso, S. and Messori, A. (1997). Relationship between cathepsin-D content and disease-free survival in node-negative breast cancer patients: a meta-analysis. *Br. J. Cancer* **76**, 661-666.

Foekens, J. A., Dall, P., Klijn, J. G., Skroch-Angel, P., Claassen, C. J., Look, M. P., Ponta, H., Van Putten, W. L., Herrlich, P. and Henzen-Logmans, S. C. (1999). Prognostic value of CD44 variant expression in primary breast cancer. *Int. J. Cancer* **84**, 209-215.

Freiss, G., Vignon, F. and Rochefort, H. (1988). Characterization and properties of two monoclonal antibodies specific for the Mr 52,000 precursor of cathepsin D in human breast cancer cells. *Cancer Res.* **48**, 3709-3715.

Garcia, M., Capony, F., Derocq, D., Simon, D., Pau, B. and Rochefort, H. (1985). Characterization of monoclonal antibodies to the estrogen-regulated Mr 52,000 glycoprotein and their use in MCF7 cells. *Cancer Res.* **45**, 709-716.

Glondu, M., Coopman, P., Laurent-Matha, V., Garcia, M., Rochefort, H. and Liaudet-Coopman, E. (2001). A mutated cathepsin-D devoid of its catalytic activity stimulates the growth of cancer cells. *Oncogene* **20**, 6920-6929.

Glondu, M., Liaudet-Coopman, E., Derocq, D., Platet, N., Rochefort, H. and Garcia, M. (2002). Down-regulation of cathepsin-D expression by antisense gene transfer inhibits tumor growth and experimental lung metastasis of human breast cancer cells. *Oncogene* **21**, 5127-5134.

Grinnell, F. (1994). Fibroblasts, myofibroblasts, and wound contraction. *J. Cell Biol.* **124**, 401-404.

Herz, J. (2006). The switch on the RAPper's necklace. *Mol. Cell* **23**, 451-455.

Herz, J. and Strickland, D. K. (2001). LRP: a multifunctional scavenger and signaling receptor. *J. Clin. Invest.* **108**, 779-784.

Heylen, N., Vincent, L. M., Devos, V., Dubois, V., Remacle, C. and Trouet, A. (2002). Fibroblasts capture cathepsin D secreted by breast cancer cells: possible role in the regulation of the invasive process. *Int. J. Oncol.* **20**, 761-767.

Hu, K., Yang, J., Tanaka, S., Gonias, S. L., Mars, W. M. and Liu, Y. (2006). Tissue-type plasminogen activator acts as a cytokine that triggers intracellular signal transduction and induces matrix metalloproteinase-9 gene expression. *J. Biol. Chem.* **281**, 2120-2127.

Hu, L., Roth, J. M., Brooks, P., Luty, J. and Karpatkin, S. (2008). Thrombin up-regulates cathepsin D which enhances angiogenesis, growth, and metastasis. *Cancer Res.* **68**, 4666-4673.

Kinoshita, A., Shah, T., Tangredi, M. M., Strickland, D. K. and Hyman, B. T. (2003). The intracellular domain of the low density lipoprotein receptor-related protein modulates transactivation mediated by amyloid precursor protein and Fe65. *J. Biol. Chem.* **278**, 41182-41188.

Koblinski, J. E., Dosescu, J., Sameni, M., Moin, K., Clark, K. and Sloane, B. F. (2002). Interaction of human breast fibroblasts with collagen I increases secretion of procathepsin B. *J. Biol. Chem.* **277**, 32220-32227.

Koong, A. C., Denko, N. C., Hudson, K. M., Schindler, C., Swiersz, L., Koch, C., Evans, S., Ibrahim, H., Le Q. T., Terris, D. J. et al. (2000). Candidate genes for the hypoxic tumor phenotype. *Cancer Res.* **60**, 883-887.

Laurent-Matha, V., Farnoud, M. R., Lucas, A., Rougeot, C., Garcia, M. and Rochefort, H. (1998). Endocytosis of pro-cathepsin D into breast cancer cells is mostly independent of mannose-6-phosphate receptors. *J. Cell Sci.* **111**, 2539-2549.

Laurent-Matha, V., Lucas, A., Huttler, S., Sandhoff, K., Garcia, M. and Rochefort, H. (2002). Procathepsin D interacts with prosaposin in cancer cells but its internalization is not mediated by LDL receptor-related protein. *Exp. Cell Res.* **277**, 210-219.

Laurent-Matha, V., Maruani-Herrmann, S., Prebois, C., Beaujouin, M., Glondu, M., Noel, A., Alvarez-Gonzalez, M. L., Blacher, S., Coopman, P., Baghdiguian, S. et al. (2005). Catalytically inactive human cathepsin D triggers fibroblast invasive growth. *J. Cell Biol.* **168**, 489-499.

Laurent-Matha, V., Derocq, D., Prebois, C., Katunuma, N. and Liaudet-Coopman, E. (2006). Processing of human cathepsin D is independent of its catalytic function and auto-activation: involvement of cathepsins L and B. *J. Biochem.* **139**, 363-371.

Li, Y., Lu, W. and Bu, G. (2003). Essential role of the low density lipoprotein receptor-related protein in vascular smooth muscle cell migration. *FEBS Lett.* **555**, 346-350.

Liaudet-Coopman, E., Beaujouin, M., Derocq, D., Garcia, M., Glondu-Lassis, M., Laurent-Matha, V., Prebois, C., Rochefort, H. and Vignon, F. (2006). Cathepsin D: newly discovered functions of a long-standing aspartic protease in cancer and apoptosis. *Cancer Lett.* **237**, 167-179.

Lillis, A. P., Mikhailenko, I. and Strickland, D. K. (2005). Beyond endocytosis: LRP function in cell migration, proliferation and vascular permeability. *J. Thromb. Haemost.* **3**, 1884-1893.

Liotta, L. A. and Kohn, E. C. (2001). The microenvironment of the tumour-host interface. *Nature* **411**, 375-379.

Masson, R., Lefebvre, O., Noel, A., Fahime, M. E., Chenard, M. P., Wendling, C., Kebers, F., LeMeur, M., Dierich, A., Foidart, J. M. et al. (1998). In vivo evidence that the stromelysin-3 metalloproteinase contributes in a paracrine manner to epithelial cell malignancy. *J. Cell Biol.* **140**, 1535-1541.

May, P., Reddy, Y. K. and Herz, J. (2002). Proteolytic processing of low density lipoprotein receptor-related protein mediates regulated release of its intracellular domain. *J. Biol. Chem.* **277**, 18736-18743.

Metcalf, P. and Fusek, M. (1993). Two crystal structures for cathepsin D: the lysosomal targeting signal and active site. *EMBO J.* **12**, 1293-1302.

Mohamed, M. M. and Sloane, B. F. (2006). Cysteine cathepsins: multifunctional enzymes in cancer. *Nat. Rev. Cancer* **6**, 764-775.

Montel, V., Gaultier, A., Lester, R. D., Campana, W. M. and Gonias, S. L. (2007). The low-density lipoprotein receptor-related protein regulates cancer cell survival and metastasis development. *Cancer Res.* **67**, 9817-9824.

Mueller, M. M. and Fusenig, N. E. (2004). Friends or foes-bipolar effects of the tumour stroma in cancer. *Nat. Rev. Cancer* **4**, 839-849.

Obermeyer, K., Krueger, S., Peters, B., Falkenberg, B., Roessner, A. and Rocken, C. (2007). The expression of low density lipoprotein receptor-related protein in colorectal carcinoma. *Oncol. Rep.* **17**, 361-367.

Rijnboutt, S., Kal, A. J., Geuze, H. J., Aerts, H. and Strous, G. J. (1991). Mannose 6-phosphate-independent targeting of cathepsin D to lysosomes in HepG2 cells. *J. Biol. Chem.* **266**, 23586-23592.

Rochefort, H. and Liaudet-Coopman, E. (1999). Cathepsin D in cancer metastasis: a protease and a ligand. *Apmis* **107**, 86-95.

Rodriguez, J., Vazquez, J., Corte, M. D., Lamelas, M., Bongera, M., Corte, M. G., Alvarez, A., Allende, M., Gonzalez, L., Sanchez, M. et al. (2005). Clinical significance of cathepsin D concentration in tumor cytosol of primary breast cancer. *Int. J. Biol. Markers* **20**, 103-111.

Slentz-Kesler, K., Moore, J. T., Lombard, M., Zhang, J., Hollingsworth, R. and Weiner, M. P. (2000). Identification of the human Mnk2 gene (MKNK2) through protein interaction with estrogen receptor beta. *Genomics* **69**, 63-71.

Song, H., Li, Y., Lee, J., Schwartz, A. L. and Bu, G. (2009). Low-density lipoprotein receptor-related protein 1 promotes cancer cell migration and invasion by inducing the expression of matrix metalloproteinases 2 and 9. *Cancer Res.* **69**, 879-886.

Strickland, D. K. and Ranganathan, S. (2003). Diverse role of LDL receptor-related protein in the clearance of proteases and in signaling. *J. Thromb. Haemost.* **1**, 1663-1670.

Vignon, F., Capony, F., Chambon, M., Freiss, G., Garcia, M. and Rochefort, H. (1986). Autocrine growth stimulation of the MCF 7 breast cancer cells by the estrogen-regulated 52 K protein. *Endocrinology* **118**, 1537-1545.

von Arnim, C. A., Kinoshita, A., Peltan, I. D., Tangredi, M. M., Herl, L., Lee, B. M., Spoelgen, R., Hshieh, T. T., Ranganathan, S., Battey, F. D. et al. (2005). The low density lipoprotein receptor-related protein (LRP) is a novel beta-secretase (BACE1) substrate. *J. Biol. Chem.* **280**, 17777-17785.

Wu, L. and Gonias, S. L. (2005). The low-density lipoprotein receptor-related protein-1 associates transiently with lipid rafts. *J. Cell Biochem.* **96**, 1021-1033.

Yang, M., Huang, H., Li, J., Li, D. and Wang, H. (2004). Tyrosine phosphorylation of the LDL receptor-related protein (LRP) and activation of the ERK pathway are required for connective tissue growth factor to potentiate myofibroblast differentiation. *FASEB J.* **18**, 1920-1921.

Zhang, H., Links, P. H., Ngsee, J. K., Tran, K., Cui, Z., Ko, K. W. and Yao, Z. (2004). Localization of low density lipoprotein receptor-related protein 1 to caveolae in 3T3-L1 adipocytes in response to insulin treatment. *J. Biol. Chem.* **279**, 2221-2230.

Zurhove, K., Nakajima, C., Herz, J., Bock, H. H. and May, P. (2008). Gamma-secretase limits the inflammatory response through the processing of LRP1. *Sci. Signal.* **1**, ra15.